

## The influence of the ion polarization current on magnetic island stability in a tokamak plasma

R. Fitzpatrick, F. L. Waelbroeck, and F. Militello

Citation: *Physics of Plasmas* (1994-present) **13**, 122507 (2006); doi: 10.1063/1.2402914

View online: <http://dx.doi.org/10.1063/1.2402914>

View Table of Contents: <http://scitation.aip.org/content/aip/journal/pop/13/12?ver=pdfcov>

Published by the [AIP Publishing](#)

---

### Articles you may be interested in

[Double tearing mode induced by parallel electron viscosity in tokamak plasmas](#)

*Phys. Plasmas* **17**, 112102 (2010); 10.1063/1.3503584

[Hypersonic drift-tearing magnetic islands in tokamak plasmas](#)

*Phys. Plasmas* **14**, 122502 (2007); 10.1063/1.2811928

[Interaction of scrape-off layer currents with magnetohydrodynamical instabilities in tokamak plasmas](#)

*Phys. Plasmas* **14**, 062505 (2007); 10.1063/1.2747624

[Island-induced bootstrap current on the saturation of a thin magnetic island in tokamaks](#)

*Phys. Plasmas* **14**, 042507 (2007); 10.1063/1.2730500

[Collisionality dependence of the polarization current caused by a rotating magnetic island](#)

*Phys. Plasmas* **12**, 072501 (2005); 10.1063/1.1937338

---



# The influence of the ion polarization current on magnetic island stability in a tokamak plasma

R. Fitzpatrick, F. L. Waelbroeck, and F. Militello

*Institute for Fusion Studies, Department of Physics, University of Texas at Austin, Austin, Texas 78712*

(Received 8 September 2006; accepted 8 November 2006; published online 19 December 2006)

The influence of the ion polarization current on the stability of a constant- $\psi$  magnetic island in a tokamak plasma is investigated numerically using a reduced two-fluid model in two-dimensional slab geometry. The polarization current is found to be negligibly small when the island is either too narrow or too wide. However, under certain circumstances, there exists an intermediate regime in which the polarization current is appreciable, and has a stabilizing influence on the island. This effect may account for the metastable nature of neoclassical tearing modes in tokamak plasmas.

© 2006 American Institute of Physics. [DOI: 10.1063/1.2402914]

## I. INTRODUCTION

### A. Background and motivation

Tearing modes are global instabilities that often limit fusion plasma performance in magnetic confinement devices, such as tokamaks, which rely on the existence of nested toroidal magnetic flux surfaces.<sup>1</sup> As the name suggests, “tearing” modes tear and reconnect magnetic field lines, in the process converting nested toroidal flux surfaces into helical magnetic islands. Such islands degrade plasma confinement because heat and particles are able to travel radially from one side of an island to another by flowing along magnetic field lines, which is a relatively fast process, instead of having to diffuse across magnetic flux surfaces, which is a relatively slow process.<sup>2</sup>

In a two-fluid plasma model,<sup>3</sup> which is far more applicable to present-day magnetic confinement devices than a conventional single-fluid model, a magnetic island is embedded within ion and electron fluids which generally flow at substantially different velocities. The island itself propagates with a phase velocity that is not necessarily the same as the velocity of either fluid. Now, if the island is strongly coupled to the ion fluid, but moves at a different velocity, then the ion fluid velocity profile will inevitably become strongly sheared in the vicinity of the island’s magnetic separatrix.<sup>4</sup> As is well known, such velocity shear generates an ion polarization current that can significantly modify the stability of the island, causing it to either grow or shrink.<sup>5</sup>

In order to determine the influence of the ion polarization current on island growth, it is necessary to know both the strength of the coupling between the island and the ion fluid, and the island propagation velocity relative to this fluid. When the island is relatively wide then the coupling is strong, causing the ion fluid to be trapped inside the island’s magnetic separatrix.<sup>4,6</sup> Moreover, viscous momentum transport forces the ion fluid inside the separatrix—and thus the island itself—to flow at the same velocity as the fluid outside the separatrix.<sup>7</sup> (This conclusion is modified if the electron fluid has a comparable perpendicular viscosity to the ion fluid—but this seems rather unlikely.) The net result is that the island is convected by the ion fluid, and there is no po-

larization current, since the island must propagate at a different velocity to the ion fluid in order for such a current to be generated. Conversely, when the island is relatively narrow then it completely decouples from the ion fluid, and is simply convected by the electron fluid.<sup>8</sup> In this case, there is also no ion polarization current, since the island has to couple with the ion fluid in order for such a current to be generated. However, under certain circumstances, there exists an intermediate regime in which the island is too wide to totally decouple from the ion fluid, but too narrow to completely trap the fluid lying within its magnetic separatrix. In this case, the island couples with the ion fluid, but does not necessarily propagate at the same velocity as this fluid. Hence, an ion polarization current is generated. It is of great importance to determine whether this current has a stabilizing or destabilizing influence on the island. If the latter is the case, then it is possible for the polarization current generated in the intermediate regime to prevent a narrow island from evolving into a wide one. On the other hand, a preexisting wide island would not experience any effect from polarization currents. Such a scenario might help to explain the mysterious metastable nature of so-called neoclassical tearing modes in tokamak plasmas.<sup>9,10</sup>

In the following, we shall investigate the effect of the ion polarization current on magnetic island stability numerically, using a reduced two-fluid plasma model in two-dimensional (2D) slab geometry.

### B. Four-field model

The model employed in this paper is a 2D slab version of the well-known four-field model.<sup>3,11</sup> This model contains electron diamagnetism, shear-Alfvén waves, drift waves, and ion acoustic waves, and is applicable to a low- $\beta$  plasma in a magnetic field dominated by a constant guide field directed along the  $z$  axis, where  $z$  is the ignorable coordinate. The model also assumes that the electron temperature is uniform, and that the ions are cold.

In the following, all lengths are normalized to some convenient length scale  $a$  (which is half the distance between the boundaries in the  $x$  direction), all magnetic field strengths to some convenient field strength  $B_0$  (which is the equilibrium

$B_y$ , at  $x=a$ ), all plasma mass densities to some convenient mass density  $\rho_0$  (which is the equilibrium mass density), and all times to the Alfvén time  $\tau_A = a\sqrt{\mu_0\rho_0}/B_0$ .

The model equations are<sup>12</sup>

$$\frac{\partial\psi}{\partial t} = [\phi - n, \psi] + \eta J, \quad (1)$$

$$\frac{\partial n}{\partial t} = [\phi, n] + \rho^2[J, \psi] + \beta[V, \psi] + D\nabla^2 n, \quad (2)$$

$$\frac{\partial U}{\partial t} = [\phi, U] + [J, \psi] + \mu\nabla^2 U, \quad (3)$$

$$\frac{\partial V}{\partial t} = [\phi, V] + [n, \psi] + \chi\nabla^2 V, \quad (4)$$

with  $U = \nabla^2\phi$  and  $J = \nabla^2\psi$ . Here,  $\psi$  is the magnetic flux function,  $\phi$  is the (normalized) electrostatic potential,  $n$  is the (normalized) perturbed plasma density,  $V$  is the (normalized) parallel ion velocity, and  $J$  (minus) is the  $z$ -directed current density. The parameter  $\rho$  is the ion Larmor radius calculated with the guide field and the electron temperature, and  $\beta$  is the conventional plasma beta calculated with the guide-field. Furthermore,  $\eta$  is the plasma resistivity,  $D$  is the particle diffusivity,  $\mu$  is the perpendicular viscosity, and  $\chi$  is the parallel viscosity. Finally,  $[A, B] \equiv \nabla A \times \nabla B \cdot \hat{z}$ . The above equations are solved in a 2D box, which is bounded in the  $x$  direction, and periodic in the  $y$  direction.

### C. Constant- $\psi$ approximation

This paper concentrates on modeling a magnetic island that lies in the so-called constant- $\psi$  regime.<sup>13</sup> In this regime, the plasma currents flowing in the immediate vicinity of the island are not strong enough to significantly affect its magnetic structure. It follows that, without sacrificing any important physics, we can simply assign the magnetic flux function the fixed value

$$\psi(x, y) = -\frac{1}{2}x^2 + \Psi \cosh(kx)\cos(ky), \quad (5)$$

where  $\Psi > 0$ , and  $k = 2\pi/L$ . The above form for  $\psi$  corresponds to a saturated, nonpropagating magnetic island, centered on the rational surface ( $x=0$ ), with a maximum separatrix width (in the  $x$  direction) of  $W = 4w$ , where  $w = \sqrt{\Psi}$ . With  $\psi$  fixed, our set of equations reduces to

$$J = -\eta^{-1}[\phi - n, \psi], \quad (6)$$

$$\frac{\partial n}{\partial t} = [\phi, n] + \rho^2[J, \psi] + \beta[V, \psi] + D\nabla^2 n, \quad (7)$$

$$\frac{\partial U}{\partial t} = [\phi, U] + [J, \psi] + \mu\nabla^2 U, \quad (8)$$

$$\frac{\partial V}{\partial t} = [\phi, V] + [n, \psi] + \chi\nabla^2 V, \quad (9)$$

$$U = \nabla^2\phi. \quad (10)$$

Note that  $\nabla^2\psi=0$ : i.e., no local currents are required to maintain the island. This implies that any currents,  $J$ , obtained from the above set of equations correspond solely to the local plasma response to the island. We expect these currents to be a combination of ion polarization currents generated by ion fluid velocity gradients, and currents associated with any net external electromagnetic force acting on the island region.<sup>14</sup>

The main advantage of specifying  $\psi$ , rather than allowing it to evolve, is that we thereby effect a clean separation between the remote plasma currents that cause the magnetic island to grow, in the first place, and the local plasma currents that develop in response to the island. In this paper, we are primarily interested in the local currents. Indeed, the remote currents are not explicitly included in our model. Another advantage of specifying  $\psi$  is that it gives us exact control over the island width,  $W$ .

### D. Unperturbed plasma state

Equations (6)–(10) are solved in a rectangular box extending from  $x=-1$  to  $x=+1$ , and from  $y=0$  to  $y=L$ . The box is periodic in the  $y$  direction. The unperturbed plasma state is

$$n = -V_*x, \quad (11)$$

$$\phi = -V_{EB}x, \quad (12)$$

with  $J=U=V=0$ . The values of all fields are fixed at  $x=\pm 1$ . Here,  $V_*$  is (minus) the unperturbed electron diamagnetic velocity, whereas  $V_{EB}$  is the unperturbed  $\mathbf{E} \times \mathbf{B}$  velocity (both in the  $y$  direction). Thus, the unperturbed ion fluid velocity is  $V_i = V_{EB}$ , and the unperturbed electron fluid velocity is  $V_e = V_{EB} - V_*$ . Note that the unperturbed electron and ion fluid velocity profiles both have zero shear.

### E. The Rutherford equation and electromagnetic forces

Let us define

$$J_c = \int_{-1}^1 \oint J \cos \theta \frac{d\theta}{\pi} dx, \quad (13)$$

$$J_s = \int_{-1}^1 \oint J \sin \theta \frac{d\theta}{\pi} dx, \quad (14)$$

where  $\theta = ky$ .

As is well known,<sup>15</sup> the quantity  $J_c$ , which measures the net ion polarization current flowing in the immediate vicinity of the island, gives rise to a modification of the conventional Rutherford island width evolution equation.<sup>16</sup> In fact, the modified Rutherford equation takes the form<sup>5</sup>

$$\frac{0.823}{\eta} \frac{dW}{dt} = \Delta' - \frac{J_c}{(W/4)^2}. \quad (15)$$

Here,  $\Delta'$  is the standard tearing stability index,<sup>13</sup> which parametrizes the influence of remote currents on the island

width evolution. Conversely, the term involving  $J_c$  parametrizes the influence of local ion polarization currents on the island evolution.

As is also well known,<sup>15</sup> the quantity  $J_s$  measures the net electromagnetic force (in the  $y$  direction) acting on the island region. In fact,

$$F_y \propto -J_s \Psi. \quad (16)$$

In this paper, we are only interested in so-called natural magnetic islands, which do not interact with any independent, externally generated, magnetic perturbations. Such islands are characterized by  $F_y=0$ .<sup>15</sup> We can set  $F_y$  to zero by adjusting the unperturbed  $\mathbf{E} \times \mathbf{B}$  velocity,  $V_{EB}$ . Once this has been achieved, the phase velocity (in the  $y$  direction) of the island in the unperturbed  $\mathbf{E} \times \mathbf{B}$  frame is simply  $V = -V_{EB}$  (since the island does not propagate in our chosen frame of reference). Note, incidentally, that a stable island phase velocity corresponds to  $dF_y/dV < 0$ .

## F. Critical parameters

In order to determine the critical parameters in our model, we need to choose a characteristic length scale, and a characteristic velocity. Obviously, the characteristic length scale for a nonlinear magnetic island is the island width,  $w$ . Likewise, the characteristic velocity is the typical flow velocity of the ion or electron fluid in the island frame, which is of order  $V_*$ . These two characteristic quantities lead to the following normalization scheme:  $x = wX$ ,  $\psi = w^2\hat{\psi}$ ,  $\phi = wV_*\hat{\phi}$ ,  $n = wV_*\hat{n}$ ,  $U = (V_*/w)\hat{U}$ ,  $V = w^2\hat{V}$ ,  $J = (V_*^2/w^2)\hat{J}$ ,  $\nabla^2 = w^{-2}\hat{\nabla}^2$ . Within this scheme, our equations are only functions of the critical parameters  $\hat{\eta} = V_*\eta/(kw^4)$ ,  $\hat{w} = w/\rho$ ,  $\hat{\beta} = w^2\beta/V_*^2$ ,  $\hat{D} = D/(w^2kV_*)$ ,  $\hat{\mu} = \mu/(w^2kV_*)$ , and  $\hat{\chi} = \chi/(w^2kV_*)$ .

The parameter  $\hat{\eta}$  measures the coupling of the electron fluid to the island. If  $\hat{\eta} \gg 1$  then resistive diffusion is sufficiently large to decouple the electron fluid from the island, and vice versa. Likewise, the parameter  $\hat{w}$  measures the coupling of the ion fluid to the island. If  $\hat{w} \ll 1$  then the island is sufficiently small that the ion fluid can decouple from it, and vice versa. The parameter  $\hat{\beta}$  measures the effectiveness of sound waves at suppressing variations of  $n$  around island flux surfaces. If  $\hat{\beta} \ll 1$  then sound waves do not propagate fast enough to prevent such variations, and vice versa. Finally,  $\hat{D}$ ,  $\hat{\mu}$ , and  $\hat{\chi}$  measure the ratios of the various perpendicular diffusion rates to the diamagnetic frequency,  $\omega_* = kV_*$ .

In this paper, we are primarily interested in magnetic islands that are sufficiently large that the electron fluid is always coupled to the island, and the various perpendicular diffusion rates are all smaller than the diamagnetic frequency. This implies that  $\hat{\eta}$ ,  $\hat{D}$ ,  $\hat{\mu}$ , and  $\hat{\chi}$  must all be  $\leq \mathcal{O}(1)$ .

Using our normalization scheme, we can write

$$J_c = -g(\hat{w}, \hat{\beta}, \hat{\eta}, \hat{D}, \hat{\mu}, \hat{\chi}) \frac{V_*^2}{w}, \quad (17)$$

where

$$g = - \int_{-\infty}^{\infty} \oint \hat{J} \cos \theta \frac{d\theta}{\pi} dX. \quad (18)$$

Thus, the Rutherford island width evolution equation becomes

$$\frac{0.823}{\eta} \frac{dW}{dt} = \Delta' + g \frac{V_*^2}{(W/4)^3}, \quad (19)$$

where the ion polarization current correction to this equation is parametrized by the  $\mathcal{O}(1)$  dimensionless quantity  $g$ . It is also convenient to parametrize the island phase velocity (in the unperturbed  $\mathbf{E} \times \mathbf{B}$  frame) in terms of the  $\mathcal{O}(1)$  dimensionless quantity

$$v = \frac{V - V_{EB}}{-V_*}. \quad (20)$$

The similarly normalized ion and electron fluid velocities (in the unperturbed  $\mathbf{E} \times \mathbf{B}$  frame) are

$$v_i(x, y) = \frac{-\phi' - V_{EB}}{-V_*}, \quad (21)$$

$$v_e(x, y) = \frac{-\phi' + n' - V_{EB}}{-V_*}, \quad (22)$$

respectively, where  $'$  denotes  $\partial/\partial x$ . Thus, the unperturbed ion and electron fluid velocity profiles are  $v_i(x)=0$  and  $v_e(x)=1$ , respectively. It follows that  $v=1$  when the island propagates with the unperturbed electron fluid, and  $v=0$  when it propagates with the unperturbed ion fluid.

## G. Island response regimes

In this paper, we shall calculate the ion polarization current parameter,  $g$ , and the island phase-velocity parameter,  $v$ , as functions of the two main plasma parameters which control the ion physics: i.e.,  $\hat{w}$  and  $\hat{\beta}$ . In fact, in a plasma with a fixed ratio of the magnetic shear length,  $L_s$ , to the density scale length,  $L_n$ , these two parameters are related via

$$\hat{\beta} = \frac{\hat{w}^2}{(L_s/L_n)^2}. \quad (23)$$

Hence, at fixed  $L_s/L_n$ , the ion physics is controlled by a single parameter: i.e.,  $\hat{w} = w/\rho$ .

From a theoretical standpoint, we can identify three different ion response regimes for the magnetic island as  $w/\rho$  is varied at fixed  $L_s/L_n$  (assuming that  $L_s/L_n \gg 1$ , as is generally the case in tokamak plasmas).

The subsonic regime corresponds to

$$\frac{L_s}{L_n} \ll \frac{w}{\rho}. \quad (24)$$

In this regime, ion acoustic waves are able to propagate around island flux surfaces sufficiently rapidly to ensure that the density is a flux-surface function: i.e.,  $n = n(\psi)$ . This inevitably leads to the flattening of the density profile inside the island separatrix.<sup>6</sup> Under these circumstances, the island becomes entrained in the ion fluid, and is forced to propagate with this fluid (given its much larger perpendicular viscosity



compared to that of the electron fluid).<sup>4</sup> This implies that  $v = 0$  in the subsonic regime. Furthermore, since the island propagates with the ion fluid, the ion fluid velocity profile remains unperturbed in the vicinity of the island.<sup>7</sup> Hence, there is no ion polarization current (since the unperturbed ion fluid velocity profile has no velocity gradients), implying that  $g = 0$  in the subsonic regime.

The hypersonic regime corresponds to

$$\frac{w}{\rho} \ll 1. \quad (25)$$

In this regime, the ion fluid completely decouples from the island.<sup>8</sup> Hence, the ion fluid flows through the island without any island-induced velocity shear. This immediately implies that there is no ion polarization current, and, hence, that  $g = 0$  in the hypersonic regime. Since the island is not coupled to the ion fluid, we expect it to propagate with the electron fluid (which remains coupled to the island). It follows that  $v = 1$  in the hypersonic regime.

Finally, the supersonic regime corresponds to

$$1 \ll \frac{w}{\rho} \ll \frac{L_s}{L_n}. \quad (26)$$

In this regime, the island is too wide to completely decouple from the ion fluid (which would cause the island to propagate with the unperturbed electron fluid), but too narrow for ion acoustic waves to totally flatten the density profile inside the separatrix (which would cause the island to propagate with the unperturbed ion fluid). Hence, we expect the island phase velocity to lie somewhere between the velocities of the unperturbed electron and ion fluids: i.e.,

$$0 < v < 1. \quad (27)$$

Moreover, it seems probable that ion fluid velocity gradients will be induced in the vicinity of the magnetic separatrix, as the ion fluid is partially dragged along by the island, giving rise to a nonzero polarization current: i.e.,  $g \neq 0$ . Clearly, it of great interest to determine whether this current is stabilizing ( $g < 0$ ) or destabilizing ( $g > 0$ ).

## H. Drift-wave emission

It is well established that a magnetic island in a two-fluid plasma emits drift waves when its phase velocity lies in the range<sup>8,17,18</sup>

$$0 < v < 1. \quad (28)$$

Such waves can affect the ion fluid velocity profile around the magnetic separatrix by transporting momentum away from the island region. As a general rule, we would expect drift-wave momentum transport to be more effective when the island propagates close to the electron fluid velocity (i.e.,  $v \rightarrow 1$ ), in which case the wavelength of the drift waves is relatively long, and they are not strongly damped by dissipative effects.<sup>19</sup> Obviously, we would also expect drift-wave momentum transport to be more effective when the plasma dissipation is reduced.

## I. Multiple solution branches

A recent publication has found multiple branches of magnetic island solutions using a reduced plasma model very similar to that employed in this paper.<sup>12</sup>

## J. Aim of paper

The aim of this paper is to determine how the ion polarization current parameter,  $g$ , and the island phase-velocity parameter,  $v$ , vary as an island moves between the hypersonic, supersonic, and subsonic regimes. As has already been mentioned, we expect to find that  $g = 0$  and  $v = 1$  in the hypersonic regime, and  $g = 0$  and  $v = 0$  in the subsonic regime. However, the expected behavior of  $g$  and  $v$  in the supersonic regime is much less clear. We also wish to clarify the effect of drift-wave emission on  $g$  and  $v$ , and to establish under what circumstances there are multiple branches of island solutions.

## II. NUMERICAL RESULTS

### A. Description of calculations

Equations (5)–(10) have been solved numerically using an initial-value, finite-difference code, which is fourth order in space, and second order in time. The code employs a fully implicit, adaptive-step, multigrid, time-stepping algorithm constructed using the Portable, Extensible Toolkit for Scientific Computing (PETSc).<sup>20</sup> All of the calculations described in this paper are performed on a  $256 \times 32$  grid. The relatively small number of grid points in the  $y$  direction is chosen to speed up the numerical calculations, but is nevertheless found to give adequate resolution.

The domain of solution is  $x = [-1, +1]$  and  $y = [0, L]$ . The initial state is  $n = -V_*x$ ,  $\phi = -V_{EB}x$ , and  $J = U = V = 0$ . The values of  $J$ ,  $n$ ,  $U$ ,  $V$ , and  $\phi$  are held constant at  $x = \pm 1$ , and the system is periodic in the  $y$  direction. The code is run until a steady state is obtained. If  $J_s \neq 0$  then the parameter  $V_{EB}$  is adjusted, and the code rerun. This process is repeated until  $J_s = 0$ : i.e., until there is zero net external electromagnetic force acting on the island region.

All of the calculations described in this paper are performed with  $\Psi = 0.01$ ,  $L = 2\pi$ , and  $V_* = 0.1$ . Thus,  $w = \sqrt{\Psi} = 0.1$ . It follows that the island lies in the hypersonic regime when  $w/\rho \ll 1$ , in the supersonic regime when  $1 \ll w/\rho \ll L_s/L_n$ , and in the subsonic regime when  $L_s/L_n \ll w/\rho$ . Hence, by varying  $\rho$  we can sweep the island across all three ion response regimes.

Note that we keep the island width fixed in our calculations, for the sake of convenience. For numerical reasons, the island needs to be sufficiently wide that it is properly resolved, but sufficiently narrow that the plasma asymptotes to its unperturbed state at the edge of the box. Thus, it is not practical to vary the island width over a large range of values—it is much more convenient to vary  $\rho$  instead. Likewise, we also keep  $\eta$ ,  $D$ ,  $\mu$ , and  $\chi$  fixed in our calculations, for the sake of convenience. These quantities need to be sufficiently small that they do not dominate the island phys-

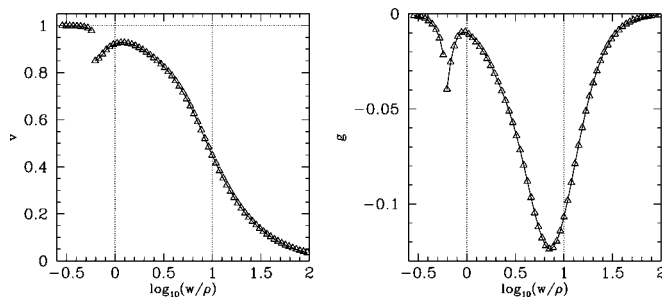


FIG. 1. The island phase-velocity parameter,  $v$ , and the ion polarization current parameter,  $g$ , calculated as functions of  $w/\rho$ . The boundaries between the subsonic and supersonic regimes ( $w/\rho=10$ ) and the supersonic and hypersonic regimes ( $w/\rho=1$ ) are indicated by the vertical dotted lines. The other calculation parameters are  $L_s/L_n=10$ ,  $V_*=0.1$ ,  $k=1$ ,  $\Psi=10^{-2}$ , and  $\eta=D=\mu=\chi=10^{-3}$ .

ics, but sufficiently large that the system can attain a steady state in a reasonable number of time steps. Thus, it is also not practical to vary  $\eta$ ,  $D$ ,  $\mu$ , and  $\chi$  over a wide range of values.

## B. Description of results

Figure 1 shows the island phase-velocity parameter,  $v$ , and the ion polarization current parameter,  $g$ , as functions of  $w/\rho$ . The calculation parameters are  $L_s/L_n=10$ ,  $V_*=0.1$ ,  $k=1$ ,  $\Psi=10^{-2}$ , and  $\eta=D=\mu=\chi=10^{-3}$ . Recall that in the subsonic regime,  $w/\rho \gg 10$ , we expect to find that  $v=0$  and  $g=0$ , whereas in the hypersonic regime,  $w/\rho \ll 0.1$ , we expect to find that  $v=1$  and  $g=0$ . It can be seen, from the figure, that these expectations are largely borne out. In the supersonic regime, the phase-velocity parameter,  $v$ , varies relatively smoothly between 0 and 1. However, the ion polarization current parameter,  $g$ , peaks in this regime, and always has a negative value. It follows that, as a magnetic island tries to grow, it passes from the hypersonic regime—in which it propagates with the electron fluid, and there is no appreciable ion polarization current—through the supersonic regime—in which it makes a transition from propagating with the electron fluid to propagating with the ion fluid, and there is a substantial stabilizing ion polarization current—to the subsonic regime—in which it propagates with the ion fluid, and there is again no appreciable ion polarization current. Clearly, it is possible for the island to be trapped in the

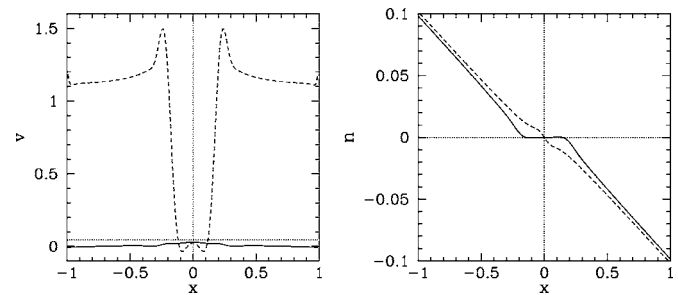


FIG. 2. Left-hand panel: The electron fluid (dashed curve) and ion fluid (solid curve) velocity profiles,  $v_e$  and  $v_i$ , through the  $O$  point, calculated for a typical subsonic island. The island-phase velocity,  $v$ , is indicated by the horizontal dotted line. The calculation parameters are  $\rho=1.25 \times 10^{-3}$ ,  $L_s/L_n=10$ ,  $V_*=0.1$ ,  $k=1$ ,  $\Psi=10^{-2}$ , and  $\eta=D=\mu=\chi=10^{-3}$ . Right-hand panel: The electron density profiles through the  $O$  (solid curve) and  $X$  points (dashed curve), calculated for the same island.

supersonic regime, and prevented from entering the subsonic regime, by the stabilizing effect of the aforementioned polarization current.

Figure 2 shows the ion and electron fluid velocity profiles through the  $O$  point, as well as the electron density profile through the  $O$  and  $X$  points, for the case of an island in the subsonic regime. Figure 3 shows the corresponding contours of the electron and ion stream-functions ( $\phi-n$  and  $\phi$ , respectively). The calculation parameters are  $\rho=1.25 \times 10^{-3}$ ,  $L_s/L_n=10$ ,  $V_*=0.1$ ,  $k=1$ ,  $\Psi=10^{-2}$ , and  $\eta=D=\mu=\chi=10^{-3}$ . It can be seen that the density is completely flattened inside the island separatrix (which extends from  $x=-0.2$  to  $x=+0.2$  for the  $O$ -point profile).<sup>11</sup> Moreover, within the separatrix, the electron and ion fluids both flow at approximately the same velocity as the island, to which they are both strongly coupled.<sup>4</sup> Finally, the island is forced to propagate with the ion fluid outside the separatrix, since the ion fluid possesses a much larger perpendicular viscosity than the electron fluid (in fact, the electron fluid only possesses a very small numerical viscosity in our simulations).<sup>7</sup> The net result is that the ion fluid velocity profile across the island is fairly flat, whereas the electron fluid velocity profile is strongly sheared inside the separatrix. The lack of shear in the ion fluid velocity profile accounts for the fact that there is very little ion polarization current in the subsonic regime.<sup>14</sup>

Figure 4 shows the ion and electron fluid velocity profiles through the  $O$  point, as well as the electron density

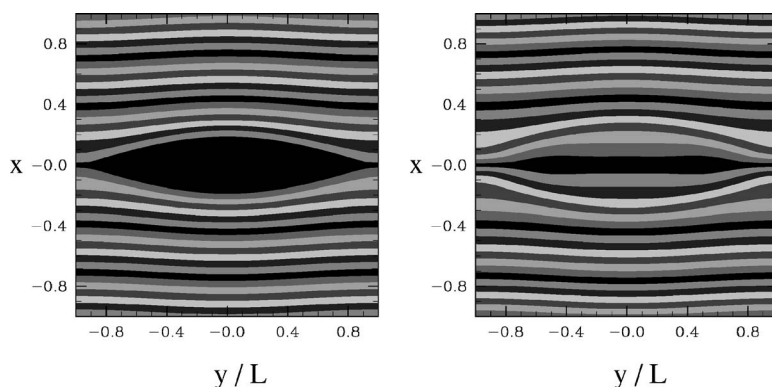


FIG. 3. Contours of the electron stream function (left-hand panel) and the ion stream function (right-hand panel) for the calculation shown in Fig. 2.

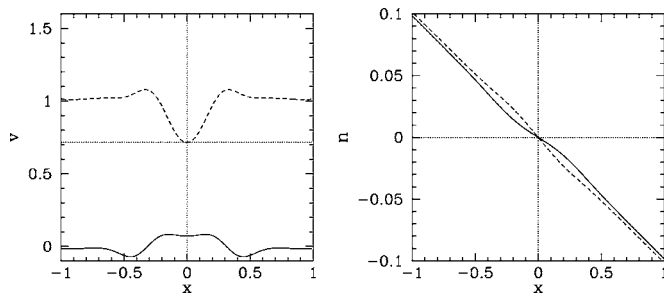


FIG. 4. Left-hand panel: The electron fluid (dashed curve) and ion fluid (solid curve) velocity profiles,  $v_e$  and  $v_i$ , through the island  $O$  point, calculated for a typical supersonic island. The island-phase velocity,  $v$ , is indicated by the horizontal dotted line. The calculation parameters are  $\rho=2 \times 10^{-2}$ ,  $L_s/L_n=10$ ,  $V_*=0.1$ ,  $k=1$ ,  $\Psi=10^{-2}$ , and  $\eta=D=\mu=\chi=10^{-3}$ . Right-hand panel: The electron density profiles through the  $O$  (solid curve) and  $X$  points (dashed curve), calculated for the same island.

profile through the  $O$  and  $X$  points, for the case of an island in the supersonic regime. Figure 5 shows the corresponding contours of the electron and ion stream functions. The calculation parameters are  $\rho=2 \times 10^{-2}$ ,  $L_s/L_n=10$ ,  $V_*=0.1$ ,  $k=1$ ,  $\Psi=10^{-2}$ , and  $\eta=D=\mu=\chi=10^{-3}$ . As expected, the density is only partially flattened inside the separatrix, since the island is too narrow for ion acoustic waves to completely iron out any density variations around island flux surfaces. However, since the electron fluid is strongly coupled to the island, whereas the ion fluid is now partially decoupled, the island propagates with the electron fluid, and slips substantially with respect to the ion fluid. Nevertheless, the residual coupling between the island and the ion fluid gives rise to an appreciable drag on the island. This drag causes the electron fluid in the vicinity of the island to be pulled backward (since it is coupled to the island), and the ion fluid to be pulled forward (in the island frame). Hence, the island phase velocity lies in between the unperturbed ion and electron fluid velocities ( $v=0$  and  $v=1$ , respectively). Moreover, the ion fluid velocity shear generated, in the immediate vicinity of the island, by the aforementioned drag gives rise to a substantial stabilizing ion polarization current.

Figure 6 shows the ion and electron fluid velocity profiles through the  $O$  point, as well as the electron density profile through the  $O$  and  $X$  points, for the case of an island in the hypersonic regime. Figure 7 shows the corresponding contours of the electron and ion stream functions. The calculation parameters are  $\rho=3.49 \times 10^{-1}$ ,  $L_s/L_n=10$ ,  $V_*=0.1$ ,

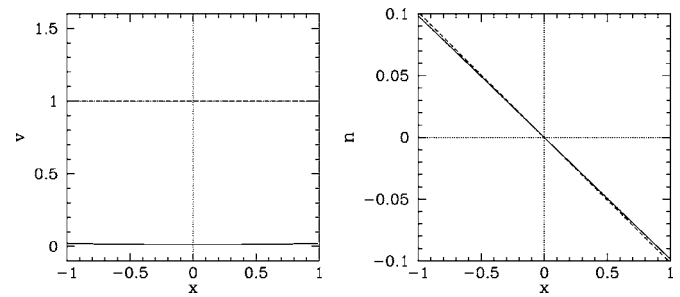


FIG. 6. Left-hand panel: The electron fluid (dashed curve) and ion fluid (solid curve) velocity profiles,  $v_e$  and  $v_i$ , through the  $O$  point, calculated for a typical hypersonic island. The island-phase velocity,  $v$ , is indicated by the horizontal dotted line (which, in this case, overlays the  $v_e$  curve). The calculation parameters are  $\rho=3.49 \times 10^{-1}$ ,  $L_s/L_n=10$ ,  $V_*=0.1$ ,  $k=1$ ,  $\Psi=10^{-2}$ , and  $\eta=D=\mu=\chi=10^{-3}$ . Right-hand panel: The electron density profiles through the  $O$  (solid curve) and  $X$  points (dashed curve), calculated for the same island.

$k=1$ ,  $\Psi=10^{-2}$ , and  $\eta=D=\mu=\chi=10^{-3}$ . As expected, the island totally decouples from the ion fluid in this regime. Hence, island has no effect on the ion fluid velocity profile. However, the island remains strongly coupled to the electron fluid. In fact, the island is simply convected by the unperturbed electron fluid, since there is no drag due to coupling with the ion fluid. It follows that there is no flattening of the density across the island, because the ion fluid stream function,  $\phi$ , and the electron fluid stream function,  $\phi-n$ , are both unperturbed. Finally, since the ion fluid velocity profile is unaffected by the island, there is no ion polarization current in the hypersonic regime.

Note that the  $v$  and  $g$  curves in Fig. 1 both exhibit small discontinuities in the hypersonic regime. There are, in fact, two branches of solutions. The first, which is termed the electron branch, connects smoothly with the solution in the extreme hypersonic regime, whereas the second, which is termed the ion branch, connects smoothly with the solution in the extreme subsonic regime. If an island on the electron branch of solutions slowly grows then this branch eventually becomes unstable (i.e.,  $dF_y/dV$  becomes positive), triggering a bifurcation to the ion branch. Likewise, if an island on the ion branch of solutions slowly shrinks then it also becomes unstable, triggering a bifurcation to the electron branch. This behavior is somewhat similar to that reported in Ref. 12. Note, also, that the  $g$  curve in Fig. 1 exhibits a small negative spike in the vicinity of the bifurcations between the two

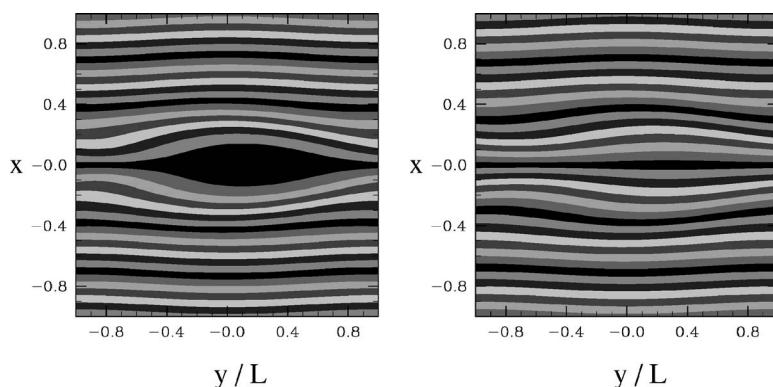


FIG. 5. Contours of the electron stream-function (left-hand panel) and the ion stream function (right-hand panel) for the calculation shown in Fig. 4.

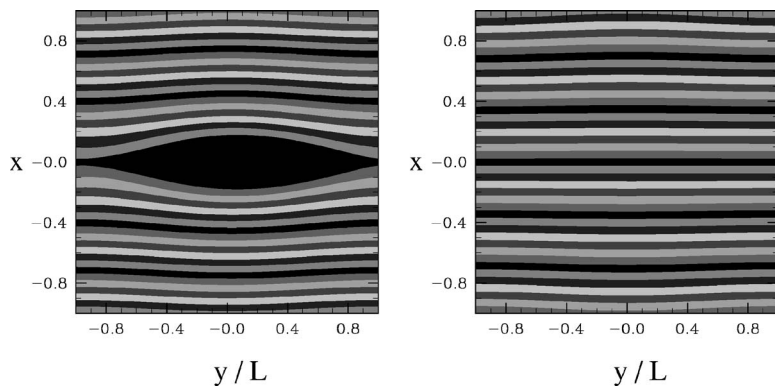


FIG. 7. Contours of the electron stream-function (left-hand panel) and the ion stream-function (right-hand panel) for the calculation shown in Fig. 6.

branches of solutions. Hence, it may be possible for a growing magnetic island to be trapped in the hypersonic regime by the stabilizing ion polarization current associated with this spike.

Figure 8 shows the same type of data as Fig. 1, calculated for a plasma with a larger value of  $L_s/L_n$ . The calculation parameters are  $L_s/L_n=100$ ,  $V_* = 0.1$ ,  $k=1$ ,  $\Psi=10^{-2}$ , and  $\eta=D=\mu=\chi=10^{-3}$ . This figure makes it clear that the large negative spike in  $g$  seen in Fig. 1 is associated with the boundary between the subsonic and supersonic regimes, whereas the small negative spike is associated with the boundary between the hypersonic and supersonic regimes.

Figure 9 also shows the same type of data as Fig. 1, calculated for a plasma with somewhat lower dissipation. The calculation parameters are  $L_s/L_n=10$ ,  $V_* = 0.1$ ,  $k=1$ ,  $\Psi=10^{-2}$ , and  $\eta=D=\mu=\chi=7.071 \times 10^{-4}$ . The main effect of reducing the plasma dissipation is to enhance any momentum transport associated with drift waves radiated by the island (since the drift waves are less strongly damped). Thus, a comparison between the curves shown in Figs. 1 and 9 should give us a rough idea of the importance of drift-wave momentum transport for islands on the two branches of solutions. The figures indicate that, for the ion branch of solutions, such momentum transport is completely negligible in the subsonic regime, becomes increasingly significant in the supersonic regime, and is fairly substantial in the hypersonic regime. On the other hand, drift-wave momentum transport has little effect on the electron branch of solutions. Inciden-

tally, Fig. 9 clearly shows that there is a small amount of hysteresis in the bifurcations between the two solution branches.

Finally, Figs. 10 and 11 show the various velocity and density profiles associated with islands on the two branches of solution just prior to a bifurcation to the other branch. The calculation parameters are  $\rho=2.075 \times 10^{-1}$ ,  $L_s/L_n=10$ ,  $V_* = 0.1$ ,  $k=1$ ,  $\Psi=10^{-2}$ ,  $\eta=D=\mu=\chi=7.071 \times 10^{-4}$ , and  $\rho=1.745 \times 10^{-1}$ ,  $L_s/L_n=10$ ,  $V_* = 0.1$ ,  $k=1$ ,  $\Psi=10^{-2}$ ,  $\eta=D=\mu=\chi=7.071 \times 10^{-4}$ , respectively. It can be seen that the ion fluid velocity profiles are slightly unusual (especially on the ion branch), in that the ion fluid seems to be pushed backward, rather than pulled forward, by the island. We speculate that this effect is due to drift waves emitted by the island transporting forward momentum from the island region to the surrounding plasma. If this is indeed the case, then the drift-wave momentum transport essentially acts as a kind of negative viscosity.

### III. SUMMARY

We have employed a reduced model of a two-fluid plasma in 2D slab geometry in order to numerically investigate the influence of the ion polarization current on the stability of a constant- $\psi$  magnetic island. Our model assumes a constant electron temperature, and cold ions.

We can identify three different regimes. The hypersonic regime corresponds to  $W \ll \rho$ , where  $W$  is the island width,

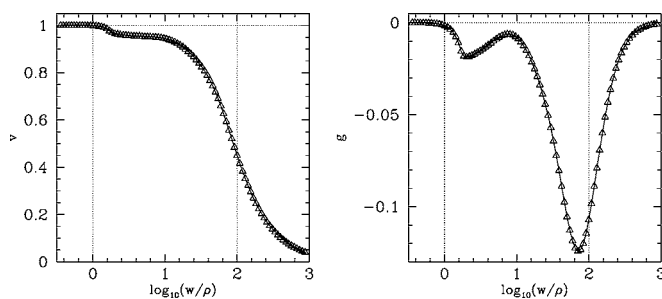


FIG. 8. The island phase-velocity parameter,  $v$ , and the ion polarization current parameter,  $g$ , calculated as functions of  $w/\rho$ . The boundaries between the subsonic and supersonic regimes ( $w/\rho=100$ ) and the supersonic and hypersonic regimes ( $w/\rho=1$ ) are indicated by the vertical dotted lines. The other calculation parameters are  $L_s/L_n=100$ ,  $V_* = 0.1$ ,  $k=1$ ,  $\Psi=10^{-2}$ , and  $\eta=D=\mu=\chi=10^{-3}$ .

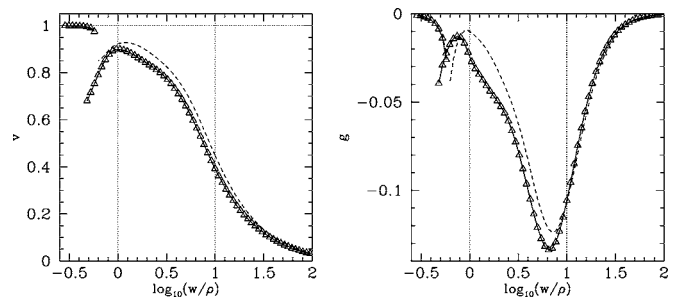


FIG. 9. The island phase-velocity parameter,  $v$ , and the ion polarization current parameter,  $g$ , calculated as functions of  $w/\rho$ . The boundaries between the subsonic and supersonic regimes ( $w/\rho=10$ ) and the supersonic and hypersonic regimes ( $w/\rho=1$ ) are indicated by the vertical dotted lines. The other calculation parameters are  $L_s/L_n=10$ ,  $V_* = 0.1$ ,  $k=1$ ,  $\Psi=10^{-2}$ , and  $\eta=D=\mu=\chi=7.071 \times 10^{-4}$ . The dashed curves show the data from Fig. 1, for the sake of comparison.



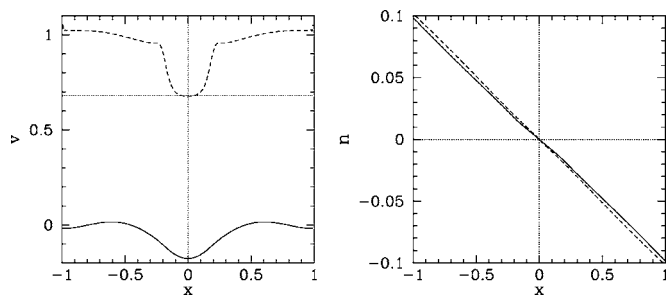


FIG. 10. Left-hand panel: The electron fluid (dashed curve) and ion fluid (solid curve) velocity profiles,  $v_e$  and  $v_i$ , through the  $O$  point, calculated for an ion branch island close to the bifurcation to the electron branch. The island-phase velocity,  $v$ , is indicated by the horizontal dotted line. The calculation parameters are  $\rho=2.075 \times 10^{-1}$ ,  $L_s/L_n=10$ ,  $V_s=0.1$ ,  $k=1$ ,  $\Psi=10^{-2}$ , and  $\eta=D=\mu=\chi=7.071 \times 10^{-4}$ . Right-hand panel: The electron density profiles through the  $O$  (solid curve) and  $X$  points (dashed curve), calculated for the same island.

and  $\rho$  the ion Larmor radius calculated with the electron temperature. The supersonic regime corresponds to  $\rho \ll W \ll (L_s/L_n)\rho$ , where  $L_s$  and  $L_n$  are the magnetic shear length, and the density scale length, respectively. (Here, we are assuming that  $L_s/L_n \gg 1$ , as is generally the case in conventional tokamak plasmas.) Finally, the subsonic regime corresponds to  $(L_s/L_n)\rho \ll W$ .

In the hypersonic regime, the ion fluid completely decouples from the island, which is convected by the electron fluid, to which it is strongly coupled. It follows that the island does not induce any shear in the ion fluid velocity profile, and so there is no ion polarization current. In the subsonic regime, both the ion and the electron fluids are strongly coupled to the island. However, since the ion fluid has a much greater perpendicular viscosity than the electron fluid, the ion fluid velocity profile across the island region remains relatively flat, whereas that of the electron fluid becomes strongly sheared. Thus, the island does not generate an ion polarization current, since it does not induce shear in the ion fluid velocity profile. Finally, in the supersonic regime, the island is strongly coupled to the electron fluid, but only weakly coupled to the ion fluid. In this case, the island moves with the electron fluid, but exerts a drag on the ion fluid. This drag induces shear in both the electron and the ion fluid velocity profiles. The latter shear generates an ion polarization current which always turns out to be stabilizing.

The fact that there is no ion polarization current in the hypersonic and subsonic regimes, but a stabilizing polarization current in the supersonic regime, gives rise to a possible scenario in which a slowly growing magnetic island can be trapped in the supersonic regime, and, thus, prevented from growing and entering the subsonic regime. If, however, the same island is somehow forced into the subsonic regime, then the stabilizing polarization current will disappear, and the island will resume its growth. Neoclassical tearing modes in tokamak plasmas often exhibit metastable behavior that is qualitatively similar to that described in this scenario.<sup>10</sup>

From Eq. (19), the critical value of  $a\Delta'$  which must be exceeded before an the island can escape from the supersonic regime [i.e., before the island width can exceed  $\rho(L_s/L_n)$ ]

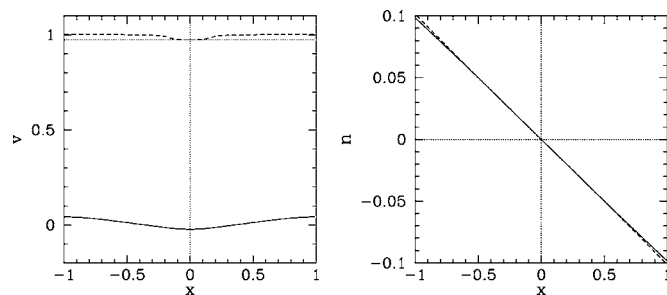


FIG. 11. Left-hand panel: The electron fluid (dashed curve) and ion fluid (solid curve) velocity profiles,  $v_e$  and  $v_i$ , through the  $O$  point, calculated for an electron branch island close to the bifurcation to the ion branch. The island-phase velocity,  $v$ , is indicated by the horizontal dotted line. The calculation parameters are  $\rho=1.745 \times 10^{-1}$ ,  $L_s/L_n=10$ ,  $V_s=0.1$ ,  $k=1$ ,  $\Psi=10^{-2}$ , and  $\eta=D=\mu=\chi=7.071 \times 10^{-4}$ . Right-hand panel: The electron density profiles through the  $O$  (solid curve) and  $X$  points (dashed curve), calculated for the same island.

scales like  $V_*^2/(\rho L_s/L_n)^3$  in normalized units. In unnormalized units, the scaling becomes  $(\beta/\rho)(L_n a^3/L_s^3)$ .

We find that there are two branches of island solution, dubbed the electron branch and the ion branch, since the island moves more with the electron fluid on the former branch than on the latter. This result is somewhat similar to that reported in Ref. 12. The electron branch only exists in the hypersonic regime, whereas the ion branch extends from the subsonic to the hypersonic regime, but does not exist in the extreme hypersonic regime. A magnetic island must make discontinuous jumps from one branch to the other as it grows or shrinks. There is a small amount of hysteresis in this process. The simultaneous existence of two branches of island solutions in the hypersonic regime seems to be associated with an effective negative viscosity generated by drift waves radiated by the island.

There are, of course, many important physical effects missing from our model. These include electron temperature gradients, ion diamagnetism, finite ion orbit widths, magnetic field-line curvature, neoclassical viscosity, and ion Landau damping. Naturally, these deficiencies need to be addressed before our model can be directly applied to tokamak experiments. Nevertheless, we feel that we have taken an important first step in understanding the influence of the ion polarization current on tearing mode stability in tokamak plasmas.

## ACKNOWLEDGMENT

This research was funded by the U.S. Department of Energy under Contract No. DE-FG05-96ER-54346.

<sup>1</sup>M. N. Rosenbluth, Plasma Phys. Controlled Fusion **41**, A99 (1999).

<sup>2</sup>Z. Chang, and J. D. Callen, Nucl. Fusion **30**, 219 (1990).

<sup>3</sup>R. Hazeltine, M. Kotschenreuther, and J. Morrison, Phys. Fluids **28**, 2466 (1985).

<sup>4</sup>R. Fitzpatrick and F. L. Waelbroeck, Phys. Plasmas **12**, 022307 (2005).

<sup>5</sup>A. I. Smolyakov, Plasma Phys. Controlled Fusion **35**, 657 (1993).

<sup>6</sup>B. D. Scott, A. B. Hassam, and J. F. Drake, Phys. Fluids **28**, 275 (1985).

<sup>7</sup>R. Fitzpatrick, P. G. Watson, and F. L. Waelbroeck, Phys. Plasmas **12**, 082510 (2005).

<sup>8</sup>F. L. Waelbroeck, Phys. Rev. Lett. **95**, 035002 (2005).

<sup>9</sup>H. R. Wilson, J. W. Connor, R. J. Hastie, and C. C. Hegna, Phys. Plasmas **3**, 248 (1996).

- <sup>10</sup>O. Sauter, R. J. Buttery, R. Felton, T. C. Hender, D. F. Howell *et al.*, *Plasma Phys. Controlled Fusion* **44**, 1999 (2002).
- <sup>11</sup>B. D. Scott, J. F. Drake, and A. B. Hassam, *Phys. Rev. Lett.* **54**, 1027 (1985).
- <sup>12</sup>M. Ottaviani, F. Porcelli, and D. Grasso, *Phys. Rev. Lett.* **93**, 075001 (2004).
- <sup>13</sup>H. P. Furth, J. Killeen, and M. N. Rosenbluth, *Phys. Fluids* **6**, 459 (1963).
- <sup>14</sup>F. L. Waelbroeck and R. Fitzpatrick, *Phys. Rev. Lett.* **78**, 1703 (1997).
- <sup>15</sup>R. Fitzpatrick and F. L. Waelbroeck, *Phys. Plasmas* **12**, 022308 (2005).
- <sup>16</sup>P. H. Rutherford, *Phys. Fluids* **16**, 1903 (1973).
- <sup>17</sup>F. L. Waelbroeck, J. W. Connor, and H. R. Wilson, *Phys. Rev. Lett.* **87**, 215003 (2001).
- <sup>18</sup>R. Fitzpatrick and F. L. Waelbroeck, *Phys. Plasmas* **12**, 122511 (2005).
- <sup>19</sup>R. D. Hazeltine and J. D. Meiss, *Plasma Confinement* (Dover, Mineola NY, 2003).
- <sup>20</sup>S. Balay, V. Eijkhout, W. D. Gropp, L. C. McInnes, and B. F. Smith, "Efficient management of parallelism in object oriented numerical software libraries," in *Modern Software Tools in Scientific Computing*, edited by E. Arge, A. M. Bruaset, and H. P. Langtangen (Birkhäuser, Boston, MA, 1997), p. 163.